

# Functional Null Mutations of *MSRB3* Encoding Methionine Sulfoxide Reductase Are Associated with Human Deafness *DFNB74*

Zubair M. Ahmed,<sup>1,2,10</sup> Rizwan Yousaf,<sup>1,4,10</sup> Byung Cheon Lee,<sup>3</sup> Shaheen N. Khan,<sup>4</sup> Sue Lee,<sup>5</sup> Kwanghyuk Lee,<sup>6</sup> Tayyab Husnain,<sup>4</sup> Atteeq Ur Rehman,<sup>4,5</sup> Sarah Bonneux,<sup>7</sup> Muhammad Ansar,<sup>8</sup> Wasim Ahmad,<sup>8</sup> Suzanne M. Leal,<sup>6</sup> Vadim N. Gladyshev,<sup>3</sup> Inna A. Belyantseva,<sup>5</sup> Guy Van Camp,<sup>7</sup> Sheikh Riazuddin,<sup>9</sup> Thomas B. Friedman,<sup>5</sup> and Saima Riazuddin<sup>1,2,\*</sup>

The *DFNB74* locus for autosomal-recessive, nonsyndromic deafness segregating in three families was previously mapped to a 5.36 Mb interval on chromosome 12q14.2-q15. Subsequently, we ascertained five additional consanguineous families in which deafness segregated with markers at this locus and refined the critical interval to 2.31 Mb. We then sequenced the protein-coding exons of 18 genes in this interval. The affected individuals of six apparently unrelated families were homozygous for the same transversion (c.265T>G) in *MSRB3*, which encodes a zinc-containing methionine sulfoxide reductase B3. c.265T>G results in a substitution of glycine for cysteine (p.Cys89Gly), and this substitution cosegregates with deafness in the six *DFNB74* families. This cysteine residue of *MSRB3* is conserved in orthologs from yeast to humans and is involved in binding structural zinc. In vitro, p.Cys89Gly abolished zinc binding and *MSRB3* enzymatic activity, indicating that p.Cys89Gly is a loss-of-function allele. The affected individuals in two other families were homozygous for a transition mutation (c.55T>C), which results in a nonsense mutation (p.Arg19X) in alternatively spliced exon 3, encoding a mitochondrial localization signal. This finding suggests that *DFNB74* deafness is due to a mitochondrial dysfunction. In a cohort of 1,040 individuals (aged 53–67 years) of European ancestry, we found no association between 17 tagSNPs for *MSRB3* and age-related hearing loss. Mouse *MsrB3* is expressed widely. In the inner ear, it is found in the sensory epithelium of the organ of Corti and vestibular end organs as well as in cells of the spiral ganglion. Taken together, *MSRB3*-catalyzed reduction of methionine sulfoxides to methionine is essential for hearing.

## Introduction

Genetic studies have uncovered numerous proteins essential for hearing.<sup>1–3</sup> Although mutations of ubiquitously expressed genes would not be expected to be associated with nonsyndromic deafness, there are now several such examples, including mutations of the genes encoding  $\gamma$ -actin (MIM 102560),<sup>4–6</sup> taperin (MIM 613354),<sup>7</sup> protocadherin-15 (MIM 605514),<sup>8</sup> tricellulin (MIM 610572),<sup>9</sup> and *DFNA5* (MIM 608798).<sup>10</sup> Given the sometimes surprising nature of the genes mutated in nonsyndromic deafness, linkage analysis performed in large families remains a powerful method for identifying components necessary for hearing. Markers at 86 distinct genetic-deafness loci that are inherited as a recessive trait (*DFNB* loci; MIM 220700) have now been linked to hearing loss in family studies. To date, the genes have been identified for only 38 of these *DFNB* loci (Hereditary Hearing Loss Homepage).<sup>1,11</sup>

Using a genome-wide linkage analysis, we mapped *DFNB74* to a 5.35 cM (5.36 Mb) interval on chromo-

some12q14.2-q15.<sup>12</sup> Recently, we ascertained an additional five families (PKDF805, PKSR3b, PKB02, 4258, and 4259) in which deafness segregated with markers at this locus. Here, we report the results of a mutation screen to identify the mutated *DFNB74* gene. We examined the coding and flanking intronic sequence of every gene in the refined linkage interval. We found two mutations (a missense null allele and a premature stop codon) in *MSRB3*, encoding methionine sulfoxide reductase B3. The missense mutation (p.Cys89Gly) segregated in six apparently unrelated *DFNB74* families, whereas the nonsense mutation (p.Arg19X) was found in two additional consanguineous Pakistani families. In vitro, studies support the hypothesis that p.Cys89Gly is also a loss-of-function allele and abolishes the enzymatic activity and Zn<sup>2+</sup> binding ability of *MSRB3*. The p.Arg19X mutation is located within alternatively spliced exon 3, encoding the mitochondrial localization signal. These suggest that one mechanism behind *DFNB74* hearing loss might be a loss of a mitochondrial function in the repair of

<sup>1</sup>Laboratory of Molecular Genetics, Division of Pediatric Otolaryngology Head & Neck Surgery, Cincinnati Children's Hospital Research Foundation, and the Department of Otolaryngology, College of Medicine, University of Cincinnati, OH, 45229 USA; <sup>2</sup>Division of Pediatric Ophthalmology, Cincinnati Children's Hospital Research Foundation, and the Department of Ophthalmology, College of Medicine, University of Cincinnati, OH, 45229 USA; <sup>3</sup>Division of Genetics, Department of Medicine, Brigham and Women's Hospital and Harvard Medical School, Boston, MA 02115, USA; <sup>4</sup>National Center of Excellence in Molecular Biology, University of the Punjab, Lahore 54500, Pakistan; <sup>5</sup>Section on Human Genetics, Laboratory of Molecular Genetics, National Institute on Deafness and Other Communication Disorders, National Institutes of Health, Rockville, MD, 20850 USA; <sup>6</sup>Department of Molecular and Human Genetics, Baylor College of Medicine, Houston, TX, 77030 USA; <sup>7</sup>Department of Medical Genetics, University of Antwerp, Universiteitsplein 1, 2610 Antwerp, Belgium; <sup>8</sup>Department of Biochemistry, Faculty of Biological Sciences, Quaid-i-Azam University, Islamabad, 45320 Pakistan; <sup>9</sup>Allama Iqbal Medical College-Jinnah Hospital Complex, University of Health Sciences, Lahore, 54500 Pakistan

<sup>10</sup>These authors contributed equally to this work.

\*Correspondence: saima.riazuddin@cchmc.org

DOI 10.1016/j.ajhg.2010.11.010. ©2011 by The American Society of Human Genetics. All rights reserved.

protein-bound and/or free methionine sulfoxides arising from oxidative stress.

## Subjects and Methods

### Family Ascertainment and Phenotype Analysis

This study was approved by institutional review board (IRB) at the National Centre of Excellence in Molecular Biology (NCEMB), Lahore, Pakistan (FWA00001758), the Combined Neuroscience IRB at the National Institutes of Health, USA (OH-93-N-016), the IRB Committee at the Cincinnati Children's Hospital Research Foundation, USA (2009-0684), the IRB at Baylor College of Medicine, Houston, TX, USA, and the IRB at Quaid-i-Azam University, Islamabad, Pakistan. Written informed consent was obtained from adult subjects and parents of minor subjects. Participating subjects were evaluated by medical-history interviews, and a physical examination was performed on two hearing-impaired individuals from each family. The degree of hearing loss was assessed by pure-tone audiometry involving air conduction (frequencies ranged from 250–8000 Hz). We assessed facial nerve function by looking for symmetrical facial expressions. Vestibular function was evaluated by tandem-gait and Romberg testing. A detailed funduscopic examination of some affected individuals ruled out frank retinopathy. Dental examinations were performed in some of the DFNB74 families so that tooth development could be evaluated. Peripheral blood samples or buccal swabs were collected from each participating subject for genomic DNA extraction.

### Candidate-Gene Screening

The 18 genes within the *DFNB74* refined linkage interval were screened for mutations by direct sequencing of PCR products generated from genomic DNA from two affected individuals of four *DFNB74* families (PKDF326, PKDF528, PKDF805, and PKDF859; Table S1, available online). Primers were designed with Primer3 software for amplification of all exons, including exon-intron boundaries, of each candidate gene. Primer pairs used for the amplification of *MSRB3* exons are listed in Table S2. Methods for direct sequencing and mutational analyses were described previously.<sup>9</sup> cosegregation of the mutations with deafness in each *DFNB74* family was confirmed by direct sequencing of the PCR products amplified from the genomic DNA of all the participating family members. Control DNA samples from ethnically matched Pakistani population were sequenced for mutant alleles in exons 3 and 4 of *MSRB3*.

### *MSRB3/Msrb3* Expression Analyses

*MSRB3* isoforms A and B (RefSeq NM\_198080.3 and NM\_001031679.2, respectively) were amplified from human multi-tissue cDNA panels (Clontech MTC human panels I and II) and from a human retina cDNA library (Genemed). The PCR primers (forward, 5'-CTGCCTGGCCTTTCCATGAG-3'; reverse, 5'-ACAATGGAGTTCCACAAACAACA-3') are located in exons 1 and 4, respectively.

*Msrb3* (RefSeq NM\_177092.4), the mouse ortholog of human *MSRB3*, was amplified from two mouse multi-tissue cDNA panels (Clontech MTC Panels I and III) and from mouse cochlear cDNA libraries that were prepared with a SMART kit and oligo-dT primers (Clontech). The PCR primers (forward, 5'-CTTTCCTCTGCTGGAGATACCAC-3'; reverse, 5'-AACGGAGTCCACAGACAACAATT-3') are located in exons 2 and 4, respectively.

For relative quantitative analysis of *Msrb3*, the PCR primers (forward, 5'-TTGTCTGTGGAACCTCCGTTG-3'; reverse, 5'-CCCCTA GGAAAAGTCATCTGTG-3') were located in exons 4 and 6, and the probe (5'-TCTGGTTCAGGCTGGC-3') spanned the junction of exons 5 and 6.

### Fluorescently Tagged *MSRB3* Expression Constructs

EGFP-tagged human *MSRB3* isoform A (IsoA\_WT) was constructed with PCR primers (forward, 5'-AGTGATGTCTGCATTCAACCTGCTG-3'; reverse, 5'-GAGCTCCGCTTTGTCTGCCTGG-3') located in exons 1a and 8, respectively, and a brain cDNA library (Clontech) was used as the source of the template. The cloned and sequence-verified product was inserted into pEGFP-N2 (Clontech). An expression vector of human *MSRB3* isoform B (IsoB\_WT) was constructed with a forward primer 5'-GCTGCCTGGCCTTTCCATGAG-3' located in exon 3 and a reverse primer 5'-GAGCTCCGCTTTGTCTGCCTGG-3' located in exon 8. Constructs encoding p.Cys89Gly mutant *MSRB3* that also included a C-terminal EGFP tag were prepared through site-directed mutagenesis for which wild-type *MSRB3* IsoA\_WT and *MSRB3* IsoB\_WT were used as templates.

### Immunoblot Analysis

For protein blot analyses, cochlea of postnatal day 7 (P7), P15, P42, and P60 C57BL/6J mice, as well as P42 vestibule, P7 heart, and P7 liver, were homogenized in ice-cold protease inhibitor cocktail (Calbiochem Biosciences) with a mechanical homogenizer (Fisher Scientific). Homogenates were boiled for 5 min in SDS-PAGE sample buffer (0.125 M Tris-HCl, 20% glycerol, 4% SDS, and 0.005% bromophenol blue). Fifty milligrams of protein in the sample was separated on a 10% Bis-Tris acrylamide gel (Invitrogen) with Novex Sharp protein standards (Invitrogen) and transferred to PVDF membrane (Millipore) for immunoblot analyses as described previously.<sup>13</sup>

### Antibodies

Antiserum raised in rabbits against human *MSRB3* was obtained from Sigma-Aldrich (HPA014432) and used for immunoblot and indirect immunofluorescence analyses. The human *MSRB3* recombinant protein epitope used for raising this commercial antiserum (100 residues) is 97% identical and 99% similar to mouse *MSRB3* (data not shown). To validate the anti-*MSRB3* antibody (HPA014432; Sigma), we performed a colocalization assay by using expression vectors encoding EGFP-tagged human and mouse *MSRB3* isoforms transfected with FuGene 6 (Roche) or by electroporation (Invitrogen) into COS7 cells. The cells were grown on coverslips in Dulbecco's modified Eagle's medium (Invitrogen) supplemented with 10% fetal bovine serum (Invitrogen). After incubation at 37°C with 5% CO<sub>2</sub> for 24 hr, transfected COS7 cells were fixed with 4% paraformaldehyde (PFA) for 20 min and permeabilized for 7 min in 0.5% Triton X-100. Nonspecific binding sites were blocked by incubation in blocking solution (2% BSA and 5% normal goat serum in PBS) for 30 min. Primary *MSRB3* antibody was diluted in blocking solution to a final concentration of ~5 mg per ml. Cells were incubated with *MSRB3* antibody for 2 hr at room temperature, and incubation with conjugated goat anti-rabbit IgG secondary antibodies (Molecular Probes) followed for 20 min. As a marker of the endoplasmic reticulum, anti-calregulin antibody (Santa Cruz) was used at a 1:500 dilution. Samples were washed in PBS, mounted with ProLong Gold Reagent (Molecular Probes), and imaged with either a Zeiss Axio

Imager Z1 microscope equipped with apotome grids or an LSM710 Zeiss confocal microscope.

For experiments involving mice, prior approval was obtained from the Animal Care and Use Committees (protocol 9B06047) at Cincinnati Children's Hospital Medical Center and at the National Institute on Deafness and Other Communication Disorders, National Institutes of Health (protocol 1263-09). Inner ears from P2 and adult C57BL6/J mice were fixed with 4% PFA at room temperature for 2 hr and washed with phosphate-buffered saline (PBS). The organs of Corti and vestibular sensory epithelia were dissected in PBS. After permeabilization with 0.5% Triton X-100 for 30 min, samples were incubated in blocking solution (5% normal goat serum and 2% bovine serum albumin [ICN] in PBS) so that the nonspecific binding sites would be blocked. Samples were then incubated for 2 hr in anti-MSRB3 antibody at ~5  $\mu\text{g}/\text{ml}$  in blocking solution. This was followed by three washes in PBS and consecutive incubation with FITC-conjugated anti-rabbit IgG secondary antibody (Molecular Probes) at 1:500 dilution and with rhodamine-phalloidin at 1:100 dilution in blocking solution for 20 min. After three washes with PBS, samples were mounted via ProLong Gold Antifade Reagent (Molecular Probes) and viewed with an LSM710 confocal microscope (Carl Zeiss Microimaging Inc.).

### Cloning, Expression, and Purification of Wild-Type and Mutant MSRB3

A construct encoding p.Cys89Gly mutant MSRB3 containing a C-terminal His tag (LEHHHHHH) was prepared through site-directed mutagenesis with the MSRB3 $\Delta$  construct that lacks sequence for residues 1–31<sup>14</sup> encoding the endoplasmic reticulum targeting sequence. The sequences of wild-type and mutant constructs were verified, and the constructs were expressed in *E. coli* BL21(DE3) and subsequently purified with a QIAGEN nickel column and concentrated with the Ultracel-10K filters (Millipore). The purity of the purified proteins was analyzed on a 3%–8% Novex-PAGE (Invitrogen).

### Determination of MSRB3 Activity and Zn Binding

The reaction mixture used for measuring the MSRB3 enzymatic activity (100  $\mu\text{l}$  in PBS [pH 7.4]) includes 20 mM dithiothreitol (DTT) and 200  $\mu\text{M}$  dabsyl-methionine-R-sulfoxide. The reaction was initiated by the addition of 5  $\mu\text{g}$  of purified wild-type or p.Cys89Gly mutant MSRB3 protein, allowed to proceed at 37°C for 30 min, and then stopped by the addition of 200  $\mu\text{l}$  of acetonitrile. After centrifugation at 4°C for 15 min at 16,200  $\times$  g, the supernatant (50  $\mu\text{l}$ ) was injected onto a C18 column (ZORBAX Eclipse XDB-C18) so that dabsyl-methionine could be quantified via HPLC as described previously.<sup>15</sup>

In order to analyze Zn binding to MSRB3, we performed elemental analysis of Zn with an inductively coupled plasma mass spectroscopy (ICP-MS) (UNL Redox Biology Center, Lincoln, NE) by using an Agilent 7500cx operating with a collision reaction cell filled with 3.5 ml/min of hydrogen and 1.5 ml/min of Argon.

### Association Studies

A set of 1040 independent samples from Belgian volunteers aged 53–67 years, collected as part of a larger study and described in detail previously,<sup>16,17</sup> was used for this study. All individuals filled in a detailed questionnaire on health and environmental factors, and individuals suffering from diseases known to affect hearing were excluded. For selected volunteers, pure-tone audiometry was performed at 0.125, 0.25, 0.5, 1, 2, 3, 4, 6, and 8 kHz for air

conduction and at 0.5, 1, 2, and 4 kHz for bone conduction. Individuals suffering from asymmetric hearing loss or conductive hearing loss were excluded. Several age- and sex-corrected audiological measures representing the hearing ability of these individuals were calculated on the basis of the pure-tone audiometry data. The measures included Z scores for high frequencies<sup>18</sup> and the three main principal components (PCs).<sup>19</sup>

$Z_{\text{high}}$  scores were calculated for the best-hearing ear as described previously.<sup>18</sup> In brief, frequency-specific thresholds were converted to sex- and age-independent Z scores based on the ISO 7029 standard. These Z scores represent the number of standard deviations that actual hearing threshold differs from the median of the standard at a given frequency. As a measure of high-frequency hearing impairment, the Z scores at 2, 4, and 8 kHz were averaged ( $Z_{\text{high}}$ ). Although  $Z_{\text{high}}$  is a good at describing an individual's hearing acuity, it ignores essential parts of the information contained in an audiogram. For instance, different audiometric shapes can result in a similar  $Z_{\text{high}}$ . The use of PCs enabled us to extract additional information, including information related to the shape of the audiogram, from the audiometric data. We performed the calculation of PCs as described previously.<sup>19</sup> Only values from six frequencies (0.250, 0.5, 1, 2, 4, and 8 kHz) from the best ear, defined as the ear with the lowest average threshold over all frequencies, were used. We removed effects of age and gender by regressing the log-transformed threshold values on age, age squared, and age cubed in males and females separately. The residuals of each regression were scaled to 1, after which values for males and females were combined. Subsequently, a classical principal-component analysis was carried out on the multivariate phenotype. We only retained the first three PCs, capturing more than 80% of the variability of the phenotype. PC1 can be considered a "size" variable, providing an overall measure of a subject's hearing ability. PC2 and PC3 should be regarded as "shape" variables. PC2 contrasts low with high frequencies and is a measure of the slope of the audiogram. PC3 contrasts the middle frequencies with the lower and higher frequencies and can be considered a measure of the concavity of an audiogram.

In order to capture most of the genetic variation of MSRB3, we selected 17 tagSNPs on the basis of the HAPMAP data of *MSRB3* by using the default setting ( $r^2 = 0.8$ ) of the Haploview's Tagger software. KBioscience (Hoddesdon Herts, UK) genotyped these SNPs by using fluorescence-based competitive allele-specific PCR (KASPar). After checking for deviation from Hardy-Weinberg equilibrium for each individual SNP, we performed an association test between  $Z_{\text{high}}$ , the three principal components, and each *MSRB3* tagSNP by using linear regression with SPSS 15.0 for Windows (SPSS inc., Chicago, Illinois, USA).

## Results

### Clinical Findings

This study reports on three Pakistani families (PKDF326, PKDF528, and PKDF859) in which profound hearing loss was found to be linked to a 5.35 cM interval on human chromosome 12q14.2-q15. The locus was designated *DFNB74*.<sup>12</sup> Subsequently, we screened genomic DNA from family members with nonsyndromic hearing loss by using microsatellite markers at the *DFNB74* locus and identified five more *DFNB74* families (PKDF805, PKB02, PKSR3b, 4258, and 4259). The affected individuals of *DFNB74*



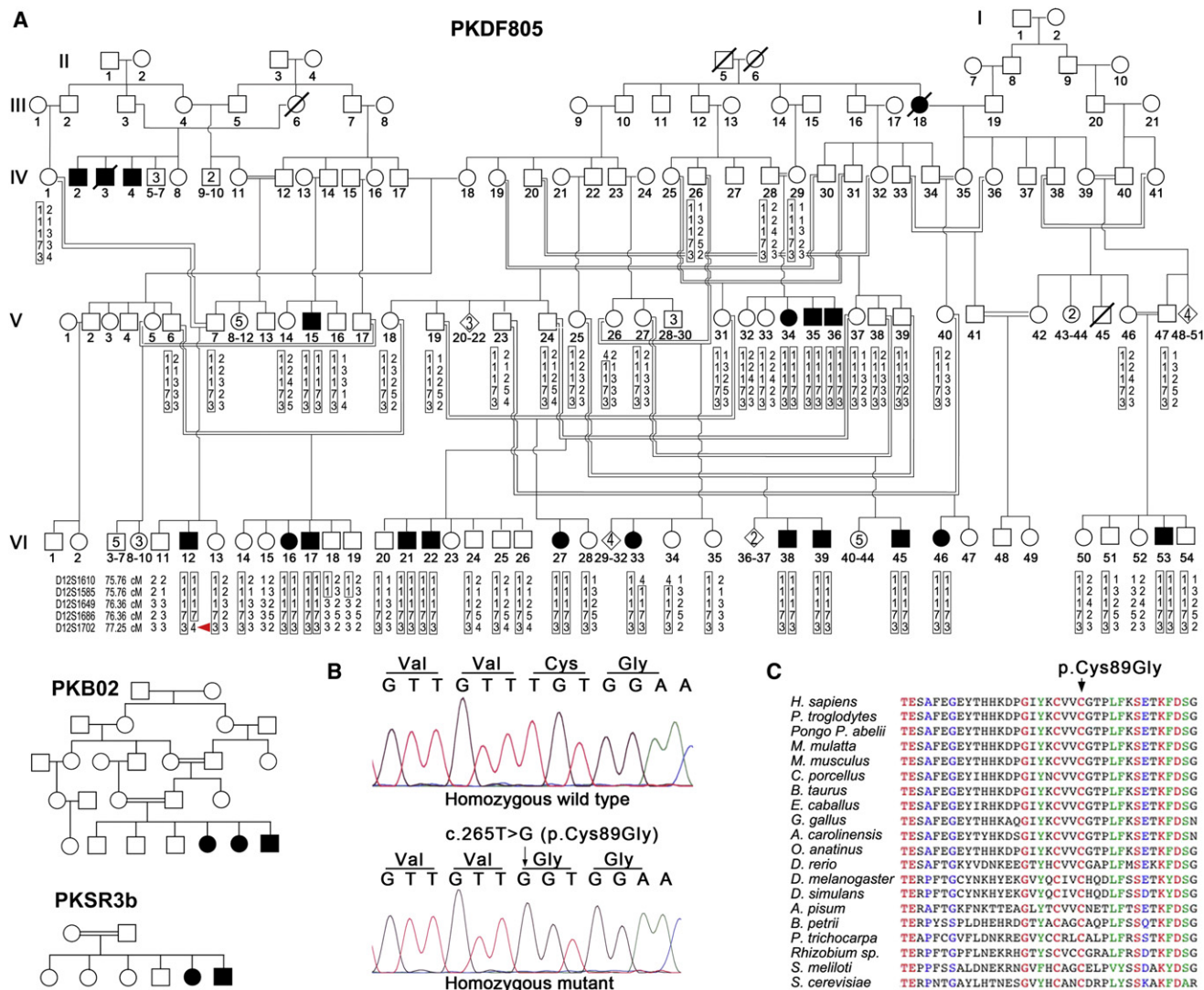


**Figure 1. Substitution of a Conserved Cysteine Residue of MSRB3 Causes Nonsyndromic Hearing Loss DFNB74**

(A) Pedigrees of three of the six DFNB74 families affected by prelingual nonsyndromic sensorineural hearing loss associated with the p.Cys89Gly alteration of MSRB3. Filled symbols represent individuals with prelingual severe to profound hearing loss, and a double horizontal line indicates a consanguineous marriage. Haplotype data for family PKDF805 (individual VI:12) provided a refined distal genetic recombination (red arrow head), and a proximal recombination breakpoint was identified in family PKDF529 (LOD 5.63, *D12S313*), as reported.<sup>12</sup>

(B) Nucleotide sequence chromatograms of part of exon 4 of *MSRB3* show the wild-type sequence and homozygosity for the c.265T>G transversion mutation.

(C) The cysteine residue at amino acid position 89 (accession number NP\_932346.1) is completely conserved across a wide variety of species. Identical residues are in red.

families, for which clinical data are available (PKDF805, PKDF859, PKDF528, PKDF326; 4258; 4259) are bilaterally profoundly deaf across all tested frequencies, and hearing loss began before the age of language acquisition. Some obligate carriers and noncarrier individuals in some of these families were tested for hearing and have normal hearing thresholds. Also, we did not observe any sign of early hearing loss in heterozygous individuals examined in our DFNB74 families. Although rigorous testing could not be done in Pakistan, vestibular function appeared normal. Other evaluations revealed no obvious skin, auricular, or dental abnormalities. Funduscopic examination of two affected individ-

uals each from families PKDF805, PKDF859, PKDF528, and PKDF326 showed no indication of retinitis pigmentosa.

### Genetic and Physical Map

Genotyping with additional STR markers and DNA samples from family PKDF528 refined the centromeric boundary of the *DFNB74* locus to *D12S1585* (75.76 cM, 63.33 Mb), and a telomeric crossover at STR *D12S1702* (77.25 cM, 65.64 Mb) was observed in affected individual VI:12 of family PKDF805 (Figure 1). If we assume locus homogeneity, these data reduced the critical linkage interval from 5.35 cM (5.36 Mb) to 1.49 cM (2.31 Mb)

(Figure 1 and Waryah et al.<sup>12</sup>). There are 18 predicted or reported genes within or adjacent to the smallest *DFNB74* linkage region: *RASSF3* (MIM 607019), *GNS* (MIM 607664), *TBC1D30*, *KIAA0984*, *AK123272*, *WIF1* (MIM 605186), *LEMD3* (MIM 607844), *MSRB3*, *RPSAP52*, *HMGA2* (MIM 600698), *AK128707*, *AY387666*, *LLPH*, *TMBIM4*, *IRAK3* (MIM 604459), *HELB*, *FLJ00057*, and *GRIP1* (MIM 604597; hg19 chr12:65,053,673–67,359,534). We sequenced the coding exons of these 18 genes along with their donor and acceptor splice sites and approximately 50 bases of flanking intronic sequences by using the genomic DNA samples from two affected individuals of each family (PKDF326, PKDF528, PKDF805, and PKDF859; LOD score above 2.5; Table S1).

### Identification of *DFNB74*

We found ten nucleotide variants in 18 candidate *DFNB74* genes, nine of which had been previously reported as single-nucleotide polymorphisms (SNPs; dbSNP build131). The only variant not present in dbSNP was c.265T>G, located in exon 4 of *MSRB3* (Figure 1B). This transversion predicts the substitution of a glycine for a conserved cysteine at residue 89 (p.Cys89Gly; Figure 1C). This missense mutation cosegregates with hearing loss in six *DFNB74* families (PKDF805, PKDF859, PKDF528, PKDF326, PKB02, and PKSR3b) and is absent in the 1000 Genomes database of human genetic variation as well as in 262 genomic DNA samples (524 control chromosomes) from normal-hearing Pakistani individuals we analyzed.

To determine whether c.265T>G segregating in these six *DFNB74* families occurs on the same haplotype, we genotyped eight SNPs distributed across the 707 kb that flank c.265T>G (Table S3). We found that all affected individuals in these six families are homozygous for the same haplotype of eight informative SNPs (Table S3), indicating that this mutation probably arose only once and is now segregating as identical by descent in apparently unrelated families.

A transition mutation (c.55C>T; NM\_001031679.2; Figure 2B) in the third exon of *MSRB3* (Figure 3A) segregates with *DFNB74* in two apparently unrelated families (4258 and 4259; Figure 2A) with suggestive linkage to markers for *DFNB74*. The mutation is predicted to replace arginine at residue 19 with a translation stop codon (p.Arg19X). This nonsense mutation cosegregates with hearing loss in both families. Haplotype analysis suggests a founder allele. c.55C>T was absent in 250 DNA samples (500 control chromosomes) from normal-hearing Pakistani individuals and in the 1000 Genomes database of human genetic variation.

### *MSRB3* and *Msrb3* Isoforms and Their Expression

We next examined the gene structure and expression of *MSRB3*. There are four alternatively spliced isoforms of human *MSRB3* (Figure 3A). Isoform A (reference sequence NM\_198080.3) has six exons encoding a protein of 192 amino acids.<sup>20</sup> Translation of isoform A begins in

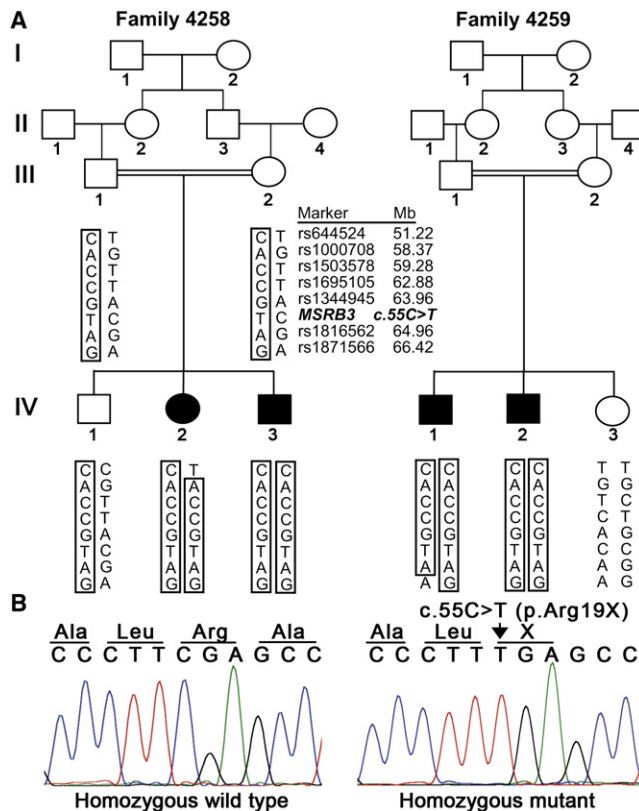


**Figure 2. Nonsense Mutation of *MSRB3* Causes Nonsyndromic Hearing Loss *DFNB74* in Two Consanguineous Pakistani Families** (A) Pedigrees of two apparently unrelated *DFNB74* families affected by prelingual nonsyndromic hearing loss due to a p.Arg19X nonsense mutation of *MSRB3*. Among the affected individuals of the two families, there is a common haplotype of SNPs spanning a 15.2 Mb region that includes *MSRB3*. Physical map positions are taken from the February 2009 (GRCh37/hg19) assembly of the Human Genome Browser. (B) Representative nucleotide sequence chromatograms of part of exon 3 of *MSRB3* show the wild-type and homozygosity for the c.55C>T (p.Arg19X) transition mutation. Mutation nomenclature is according to *MSRB3* isoform B (accession number NM\_001031679.2). Exon 3 is alternatively spliced and is absent from isoform A (Figure 3A), the longest transcript of *MSRB3* (accession number NP\_932346.1).

exon 1a (Figure 3A). The amino terminus of *MSRB3* isoform A has a predicted endoplasmic reticulum localization signal (residues 1–31), whereas the remaining peptide encodes a methionine sulfoxide reductase (Msr domain) that catalyzes the reduction of oxidized methionine residues and thus repairs oxidatively damaged proteins.<sup>21</sup>

*MSRB3* isoforms B, C, and D (NM\_001031679.2, NM\_001193460.1, and NM\_001193461.1, respectively) include cassette exon 3, which contains a translation initiation codon (Figure 3A). RNAs of isoforms B and C have in-frame stop codons upstream of the translation initiation codon in cassette exon 3. Transcription of isoform D begins in the isoform-D-specific exon 1b (Figure 3A). Isoforms B, C, and D each encode a 185 amino acid protein (NP\_001026849.1) that differs from isoform A only at its N terminus (Figure S1). Isoforms B, C, and D have an

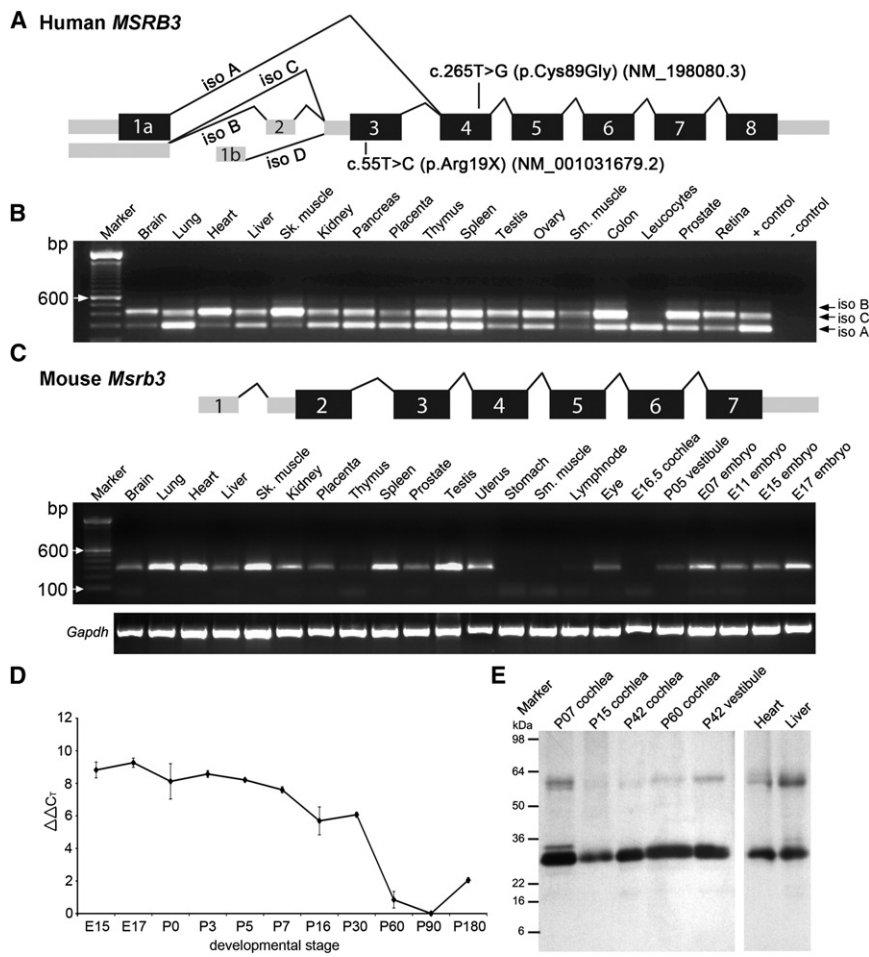


**Figure 3. Transcripts Encoding MSRB3 in Human and Mice and Their Expression Profile**

(A) Alternative splicing leads to four isoforms of human *MSRB3*. *MSRB3* isoform A has translation initiation codon (AUG) in exon 1a, which is spliced with exons 4 through 8 to encode a polypeptide of 192 amino acids. *MSRB3* isoform C includes exons 1a, 3, and 4–8. The predicted translation initiation codon for *MSRB3* isoform C is located in exon 3. The predicted open reading frame for this isoform encodes 185 amino acid residues. *MSRB3* isoform B transcript has all eight exons and utilizes the translation initiation codon present in exon 3 and also encodes the same protein of 185 amino acids. *MSRB3* isoform D utilizes cassette exon 1b and encodes a 185 amino acid polypeptide that is identical to that encoded by isoforms B and C. Shown also are the two mutations found in DFNB74 families. The numbering of the position of mutation c.265T>G (p.Cys89Gly) is based on accession number NM\_198080.3, whereas c.55C>T (p.Arg19X) is assigned on the basis of *MSRB3* isoform B (NM\_001031679.2).

(B) Human *MSRB3* isoforms A, B, and C are expressed in many tissues.

(C) Mice have only a single *Msrb3* transcript, which is ubiquitously expressed.

(D) Real-time quantitative RT-PCR analysis of *Msrb3* mRNA level in C57BL/6J mouse temporal bones at 11 different developmental stages.  $C_T$  is the observed threshold number of PCR cycles required

for detection of the amplification product;  $\Delta C_T$  is the calculated difference in  $C_T$  between the *Msrb3* gene and an internal control standard (*Gapdh*) measured in the same sample.  $\Delta\Delta C_T$  is the calculated difference in  $\Delta C_T$  between the experimental and P90 time points. (E) Sigma-Aldrich commercial antiserum raised against human *MSRB3* was used for determining the expression of mouse *MSRB3* in immunoblot analysis.

identical N terminus that is encoded by exon 3. These isoforms contain a predicted mitochondrial localization signal also encoded by exon 3, whereas the remainder of the protein is identical to isoform A (Figure S1).

The c.265T>G mutation alters all four isoforms of *MSRB3*. From these data, we can conclude that the ER or mitochondrial form of *MSRB3*, or both, is required for normal hearing. However, in exon 3 the c.55C>T mutation, predicted to be a nonsense mutation (p.Arg19X), alters isoforms B, C, and D (Figure 3A), but not isoform A, indicating that *MSRB3* isoforms targeted to mitochondria are essential for hearing. *MSRB3* isoforms A and C are easily detected in cDNA samples prepared from 17 different human tissues (Figure 3B).

In comparison to human *MSRB3*, mouse *Msrb3* has six coding exons and, from our data from multiple mouse tissue cDNAs, appears to express only a single isoform (Figure 3C). Mouse *MSRB3* has adjacent sequences for both ER and mitochondrial localization, and yet it is largely targeted to the ER for unknown reasons.<sup>14</sup> Mouse *MSRB3* is 91% identical and 94% similar to human *MSRB3* isoform B (Figure S1).

We assayed expression of C57BL/6J *Msrb3* mRNA by using a TaqMan probe and real-time quantitative RT-PCR of RNA extracted from temporal bones of embryonic day 15 (E15), E17, postnatal day 0 (P0), P3, P5, P7, P16, P30, P60, P90, and P180 mice (Figure 3D). Compared to *Gapdh* mRNA used as an internal control, *Msrb3* mRNA is easily detectable from E15 to P30, whereas expression appears to decrease after P30 but is still present in the mouse inner ear at P180 (Figure 3D).

#### Localization of MSRB3 in the Mouse Inner Ear

The specificity of *MSRB3* antibody was validated in heterologous cells that overexpress EGFP-tagged full-length human isoform A or B (Figure S3) and by immunoblot analyses (Figure 3E). *MSRB3* antibody recognizes wild-type EGFP-tagged human isoforms but does not reveal a detectable level of endogenous *MSRB3* in COS7 cells (Figure S2, arrows). Next, we immunostained the COS7 cells transiently expressing EGFP-tagged full-length wild-type human *MSRB3* and p.Cys89Gly mutant *MSRB3* isoforms with anti-*MSRB3* antibodies. At the light microscopy level we did not find a difference in the localization of



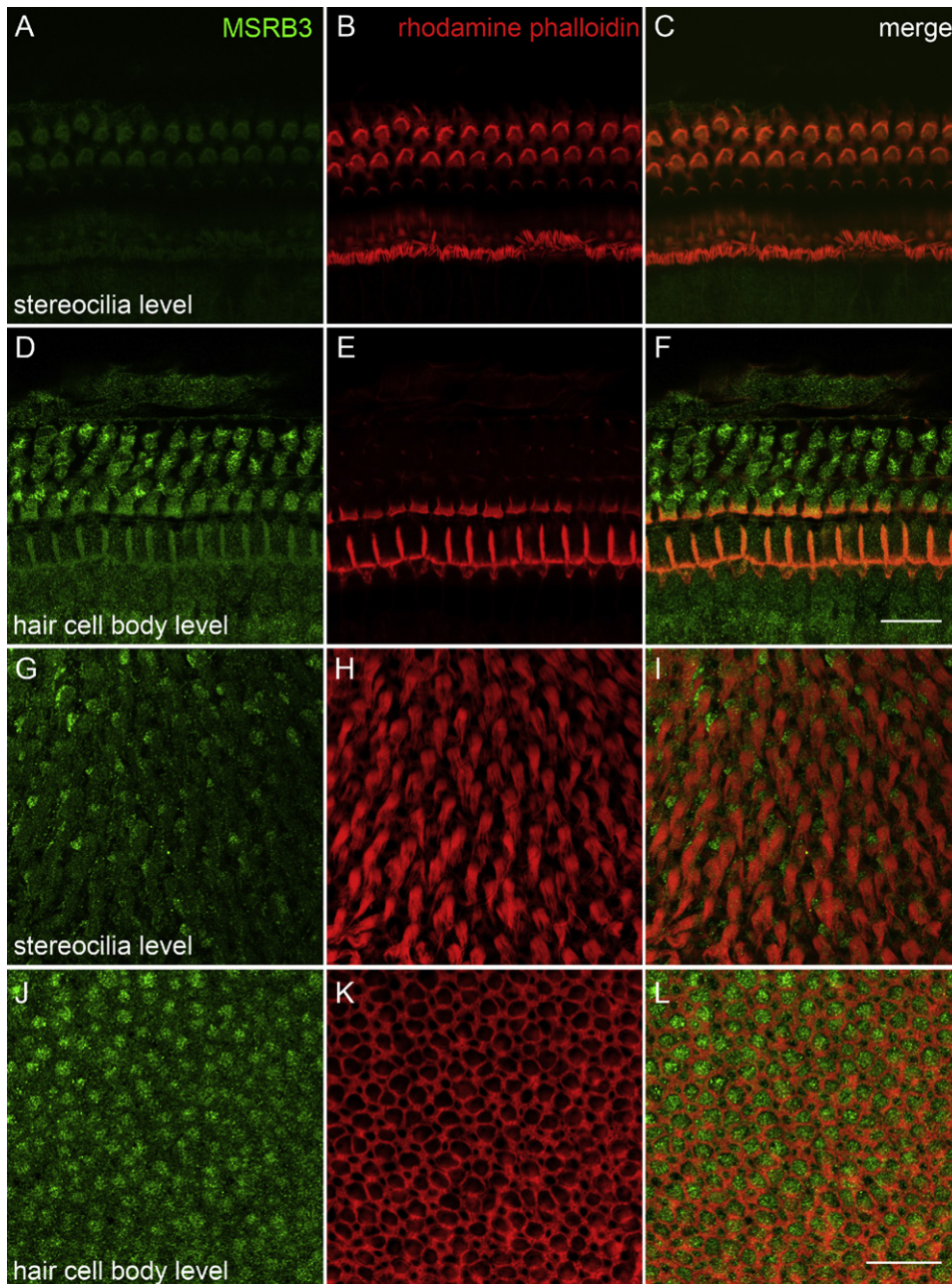


**Figure 4. MSRB3 Is Localized in the Auditory and Vestibular Sensory Epithelia of the Inner Ear**

(A and D) MSRB3 (green) is localized to the outer (OHCs) and inner (IHCs) hair cell bodies. A barely detectable level of MSRB3 was observed in the hair cell stereocilia. Supporting cells have weaker staining by anti-MSRB3 antibody than hair cells.

(B, E, H, and K) The actin cytoskeleton of the organ of Corti and vestibular sensory epithelia cells is highlighted by rhodamine-phalloidin (red).

(C, F, I, and L) Merged images.

(G and J) MSRB3 localizes in the vestibular hair cell bodies and also in supporting cells (green). Panel G shows staining at the stereocilia level. Stereocilia bundle staining is barely detectable, and a weak signal could be observed in the kinocilia (G and I). Note that the MSRB3 signal in hair cells is prominent (J and L). Scale bars in F and L are 20  $\mu$ m.

the wild-type and mutant (c.265T>G) of either the mitochondrial or the ER isoforms of human MSRB3 (Figure S3).

Immunolocalization of MSRB3 was examined in the C57BL/6J mouse organ of Corti and vestibular sensory epithelium (Figures 4A–4L). Immunoreactivity was found in the sensory epithelia of the organ of Corti and vestibular end organs as early as P2 and was detectable in adult mice

(Figures 4A, 4D, 4G, and 4J). In the organ of Corti, MSRB3 was present in inner and outer hair cells and, to a lesser extent, in supporting cells. In hair cells, MSRB3 immunofluorescence was distributed throughout the cell body (Figures 4D and 4F), and there was a barely detectable level in stereocilia (Figure 4A). MSRB3 immunoreactivity was also observed in spiral ganglion neurons (Figures S4A–S4D).

No detectable level of expression was observed in the stria vascularis when this antibody was used (data not shown). In the vestibular end organs, MSRB3 was found throughout the sensory epithelium, but more intense expression was observed in hair cells than in supporting cells (Figures 4J and 4L). In vestibular hair cells, the most prominent MSRB3 staining was present within cell bodies (Figures 4J and 4L), and a weaker signal was observed in kinocilia. MSRB3 staining in stereocilia was barely detectable (Figures 4G and 4I). No specific immunoreactivity was observed when the primary antibody was omitted.

#### p.Cys89Gly Ablates Zn Binding and Enzymatic Activity

To determine the effect of p.Cys89Gly on Zn binding and enzymatic activity, we expressed in *E. coli* the full-length wild-type and p.Cys89Gly mutant human MSRB3 without the signal sequence, purified the proteins by using a C-terminal His tag, and measured enzymatic conversion of dabsyl-methionine-*R*-sulfoxide to dabsyl-methionine in the presence of dithiothreitol (DTT).<sup>22</sup> In comparison to wild-type MSRB3, p.Cys89Gly virtually eliminated all enzymatic activity and Zn<sup>2+</sup> binding ability of MSRB3 (Figures 5A and 5B).

#### MSRB3 and Age-Related Hearing Loss

Interestingly, early-onset, rapidly progressing hearing loss in A/J mice (*ahl4*) was mapped to chromosome 10 in a region of conserved synteny with the *DFNB74* locus. We suggested that *ahl4* and *DFNB74* might result from mutations of orthologous genes.<sup>23</sup> Bioinformatic analyses of genomic sequences of *Msrb3* exons, 50 bp of flanking introns, and approximately 5,000 bp upstream of exon 1 in ten inbred mouse strains including A/J did not reveal an A/J (*ahl4*)-specific variant of *Msrb3*, indicating that an alteration of *Msrb3* is probably not responsible for the murine *ahl4* phenotype.<sup>23</sup>

We next explored the possibility that a variant associated with human *MSRB3* might make a significant contribution to age-related hearing loss (AHL). Sixty percent of people between the ages of 71 and 80 have some hearing loss.<sup>24</sup> AHL is the most common sensory disorder in the elderly and is considered a complex phenotype, but the responsible heritable and nonheritable components are not well quantified. Recent association studies have provided candidate intervals for further studies.<sup>25,26</sup>

Considering the role of methionine sulfoxide reductases in aging and age-related disorders, we hypothesized that *MSRB3* variants might be involved in AHL, and we tested this hypothesis with an association study. We analyzed 1,040 Belgian volunteers aged 53–67 years who were ascertained as part of a larger study described previously.<sup>16,17</sup> Several audiological measures representing the hearing ability of these individuals, corrected for age and sex, were calculated on the basis of pure-tone audiometry. The measures included Z scores for high frequencies<sup>18</sup> and the three main principal components, which account for

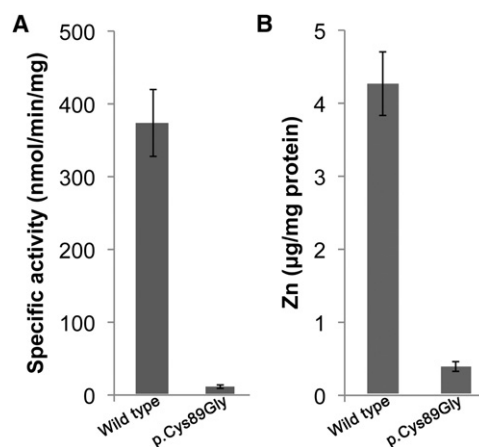


**Figure 5. Replacement of a Highly Conserved Cysteine Residue at Position 89 with Glycine Diminishes the Enzymatic Activity as Well as the Zn-Binding Ability of MSRB3**

A construct encoding mutant p.Cys89Gly human MSRB3 containing a C-terminal His tag (LEHHHHHH) was prepared through site-directed mutagenesis with a MSRB3Δ (1–31 amino acid) construct that lacked the endoplasmic-reticulum-targeting sequence.<sup>20</sup>

(A) Catalytic activity of the p.Cys89Gly mutant form of MSRB3 is shown and compared to the activity of the wild-type protein. Virtually no activity of the p.Cys89Gly mutant of MSRB3 was detected in the DTT-dependent reaction.

(B) A statistically significant reduction in Zn content of the protein was observed for p.Cys89Gly mutant MSRB3 as compared to the wild-type protein.

Data are represented as means, and error bars represent standard deviations. Error bars and standard deviation were calculated on the basis of three independent experiments.

85% of the variance.<sup>19</sup> We selected these individuals to represent the 20% extremes at both ends of the distribution for each of the three principle components from a larger set of individuals to maximize the power of the analysis. In order to capture most of the genetic variation of *MSRB3*, we selected 17 tagSNPs based on the HAPMAP data of *MSRB3* by using the default setting ( $r^2 = 0.8$ ) of the Haploview's Tagger software. We performed an association test by using linear regression with SPSS 15.0 for Windows (SPSS inc., Chicago, Illinois, USA). The analyses of Z scores and principal components showed no significant association for any of the *MSRB3* SNPs (Table S4). Although mutations of *MSRB3* cause an autosomal-recessive Mendelian form of nonsyndromic deafness, our data do not support a major role for *MSRB3* as a cause of human AHL in 53- to 67-year-old individuals of European origin.

#### Discussion

Methionine sulfoxide reductases (Msr) catalyze the repair of oxidized methionine in proteins by reducing methionine sulfoxides (Met-SO) to the corresponding methionines, thus preserving the biological activity of proteins after oxidative damage due to reactive oxygen species.<sup>21</sup> MSRB3 stereospecifically reduces methionine-*R*-sulfoxide (Met-*R*-SO) to methionine.<sup>27,28</sup> Malfunctions due to a



mutation in *MSRB3* might cause accumulation of oxidatively damaged proteins and reactive oxygen species (ROS), which in turn might activate caspases and initiate apoptosis or programmed cell death.<sup>29</sup> Apoptosis plays an essential role in normal development, morphogenesis, and tissue homeostasis throughout the body, including the inner ear.<sup>29–31</sup> Mice homozygous for a targeted deletion of caspase 3 display rapid hearing loss and profound deafness by P30 as a result of the degeneration of inner and outer hair cells and neurons in the spiral ganglion.<sup>30</sup>

Oxidative damage of proteins has been implicated in normal aging and a variety of neurodegenerative age-related diseases.<sup>32–37</sup> A role for *MSRA* in the pathogenesis of Alzheimer (MIM 104300) and Parkinson (MIM 168600) diseases has been proposed.<sup>33,35,38</sup> Furthermore, it has been suggested that oxidative damage and mitochondrial dysfunction have a role in the pathogenesis of cataracts (MIM 212500) and age-related macular degeneration (MIM 603075).<sup>39–43</sup> Although we did not observe any association between 17 tagSNPs for *MSRB3* and age-related hearing loss in a cohort 1,040 50- to 70-year old individuals of European ancestry, we do show that a recessive nonsense mutation of *MSRB3* causing deafness ablates the mitochondrial targeted isoform of *MSRB3*, whereas a missense mutation is a null allele for all isoforms of *MSRB3*.

The c.265T>G mutation of *MSRB3* results in the substitution of glycine for the cysteine at amino acid residue 89. This cysteine residue corresponds to p.Cys54 of *Drosophila* and p.Cys48 of *E. coli*. Substitution of p.Cys54 in *Drosophila* and p.Cys48 in *E. coli* *MSRB3* resulted in a complete loss of metal binding and catalytic activity.<sup>44,45</sup> These studies suggest that the introduction or removal of Zn<sup>2+</sup> in *MSRB* changes protein structure, which in turn modulates catalytic activity and thermal stability.<sup>45</sup> Therefore, we hypothesized that the *DFNB74* mutation alters or ablates zinc binding and eliminates reductase activity of this enzyme.<sup>44,45</sup>

The c.55C>T mutation found in two *DFNB74* families results in a premature translation stop codon (p.Arg19X). This mutation is present within exon 3, encoding the mitochondrial localization signal of isoforms B, C, and D, indicating that at least one of the mitochondrial targeted isoforms of *MSRB3* is essential for hearing in humans. There is another example wherein mutations of a nuclear-encoded gene altering mitochondrial function result in hearing loss. X-linked recessive mutations of *TIMM8A* are associated with deafness-dystonia-optic atrophy syndrome (Mohr-Tranebjaerg syndrome, MIM 300356), characterized by deafness, myopia, constriction of the visual field, and dystonia. Mutations of *TIMM8A* alter a nuclear-encoded mitochondrial inner-membrane complex essential for protein-import into mitochondria.<sup>46–49</sup>

In summary, an in vitro assay revealed that p.Cys89Gly completely abolished *MSRB3* enzymatic activity and that p.Arg19X is a null allele for *MSRB3* mitochondrial isoforms, indicating that *DFNB74* deafness might be a mitochondrial disease limited to the inner ear. Despite the

expression of *MSRB3* isoforms in many cell types beyond the inner ear, null alleles of *MSRB3* appear to be associated only with nonsyndromic hearing loss. How some cells compensate for the absence of *MSRB3* function is an unanswered question. An animal model will be needed to reveal the exact pathophysiological causes of deafness due to null alleles of *MSRB3* as well as the mechanism by which many cells escape the absence of functional *MSRB3*.

### Supplemental Data

Supplemental Data include four figures and four tables and can be found with this article online at <http://www.cell.com/AJHG/>.

### Acknowledgments

We wish to thank all participants in this study. We thank Shannon Bell for technical assistance and Dennis Drayna and Karen Friderici for critiques of the manuscript. This work was supported by Cincinnati Children's Hospital Research Foundation (CCHMC) intramural research funds to SR and ZA, the National Institute on Deafness and Other Communication Disorders, National Institutes of Health (NIDCD/NIH) research grant R00-DC009287-03, a Career Development Award from Research to Prevent Blindness (to Z.A.), and National Institute on Aging, NIH grant AG021518 (to V.N.G.). S. B. is a fellow of the Research Foundation Flanders (FWO-Vlaanderen). Work in Pakistan was supported by the Higher Education Commission to S.R. (Lahore); funding from World Health Organization Regional Office for the Eastern Mediterranean (EMRO) and COMSTECH (Organization of the Islamic Conference [OIC] Standing Committee on Scientific and Technological Cooperation) and from the Ministry of Science and Technology (MoST) to S.R. (Lahore); the International Center for Genetic Engineering and Biotechnology, Trieste, Italy under project CRP/PAK08-01 contract no. 08/009 to S.R. (Islamabad). Part of the work was funded by the Higher Education Commission (HEC), Government of Pakistan, and the NIH National Institute of Deafness and other Communication Disorders grant DC03594 to S.M.L. Genotyping services were partially provided by the Center for Inherited Disease Research (CIDR). CIDR is fully funded through a federal contract from the NIH to The Johns Hopkins University, contract number N01-HG-65403. Work at NIDCD/NIH was supported by intramural funds DC00039-14 to T.B.F.

Received: September 29, 2010

Revised: November 12, 2010

Accepted: November 18, 2010

Published online: December 23, 2010

### Web Resources

The URLs for data presented herein are as follows:

dbSNP homepage, <http://www.ncbi.nlm.nih.gov/SNP/>  
GenBank, <http://www.ncbi.nlm.nih.gov/Genbank/index.html>  
Haploview, <http://www.broad.mit.edu/mpg/haploview/>  
Hereditary Hearing Loss homepage, <http://hereditaryhearingloss.org/>  
Kbiosciences, <http://www.kbioscience.co.uk/>  
National Center for Biotechnology Information (NCBI), <http://www.ncbi.nlm.nih.gov/>  
Online Mendelian Inheritance in Man (OMIM), <http://www.ncbi.nlm.nih.gov/Omim/>

Primer3, <http://www.bioinformatics.nl/cgi-bin/primer3plus/primer3plus.cgi>  
UCSC human genome browser, <http://genome.cse.ucsc.edu/cgi-bin/hgGateway>  
1000 Genomes database, <http://www.1000genomes.org/page.php>

## References

1. Friedman, T.B., and Griffith, A.J. (2003). Human nonsyndromic sensorineural deafness. *Annu. Rev. Genomics Hum. Genet.* **4**, 341–402.
2. Frolenkov, G.I., Belyantseva, I.A., Friedman, T.B., and Griffith, A.J. (2004). Genetic insights into the morphogenesis of inner ear hair cells. *Nat. Rev. Genet.* **5**, 489–498.
3. Morton, C.C., and Nance, W.E. (2006). Newborn hearing screening—A silent revolution. *N. Engl. J. Med.* **354**, 2151–2164.
4. Belyantseva, I.A., Perrin, B.J., Sonnemann, K.J., Zhu, M., Stepanyan, R., McGee, J., Frolenkov, G.I., Walsh, E.J., Friderici, K.H., Friedman, T.B., and Ervasti, J.M. (2009). Gamma-actin is required for cytoskeletal maintenance but not development. *Proc. Natl. Acad. Sci. USA* **106**, 9703–9708.
5. Perrin, B.J., Sonnemann, K.J., and Ervasti, J.M. (2010). beta-actin and gamma-actin are each dispensable for auditory hair cell development but required for stereocilia maintenance. *PLoS Genet.* **6**, e1001158.
6. Zhu, M., Yang, T., Wei, S., DeWan, A.T., Morell, R.J., Elfenbein, J.L., Fisher, R.A., Leal, S.M., Smith, R.J., and Friderici, K.H. (2003). Mutations in the gamma-actin gene (ACTG1) are associated with dominant progressive deafness (DFNA20/26). *Am. J. Hum. Genet.* **73**, 1082–1091.
7. Rehman, A.U., Morell, R.J., Belyantseva, I.A., Khan, S.Y., Boger, E.T., Shahzad, M., Ahmed, Z.M., Riazuddin, S., Khan, S.N., and Friedman, T.B. (2010). Targeted capture and next-generation sequencing identifies C9orf75, encoding taperin, as the mutated gene in nonsyndromic deafness DFNB79. *Am. J. Hum. Genet.* **86**, 378–388.
8. Ahmed, Z.M., Riazuddin, S., Bernstein, S.L., Ahmed, Z., Khan, S., Griffith, A.J., Morell, R.J., Friedman, T.B., and Wilcox, E.R. (2001). Mutations of the protocadherin gene PCDH15 cause Usher syndrome type 1F. *Am. J. Hum. Genet.* **69**, 25–34.
9. Riazuddin, S., Ahmed, Z.M., Fanning, A.S., Lagziel, A., Kitajiri, S., Ramzan, K., Khan, S.N., Chattaraj, P., Friedman, P.L., Anderson, J.M., et al. (2006). Tricellulin is a tight-junction protein necessary for hearing. *Am. J. Hum. Genet.* **79**, 1040–1051.
10. Van Laer, L., Huizing, E.H., Verstreken, M., van Zuijlen, D., Wauters, J.G., Bossuyt, P.J., Van de Heyning, P., McGuirt, W.T., Smith, R.J., Willems, P.J., et al. (1998). Nonsyndromic hearing impairment is associated with a mutation in DFNA5. *Nat. Genet.* **20**, 194–197.
11. Petit, C., and Richardson, G.P. (2009). Linking genes underlying deafness to hair-bundle development and function. *Nat. Neurosci.* **12**, 703–710.
12. Waryah, A.M., Rehman, A., Ahmed, Z.M., Bashir, Z.H., Khan, S.Y., Zafar, A.U., Riazuddin, S., and Friedman, T.B. (2009). DFNB74, a novel autosomal recessive nonsyndromic hearing impairment locus on chromosome 12q14.2–q15. *Clin. Genet.* **76**, 270–275.
13. Ahmed, Z.M., Riazuddin, S., Ahmad, J., Bernstein, S.L., Guo, Y., Sabar, M.F., Sieving, P., Griffith, A.J., Friedman, T.B., Belyantseva, I.A., and Wilcox, E.R. (2003). PCDH15 is expressed in the neurosensory epithelium of the eye and ear and mutant alleles are responsible for both USH1F and DFNB23. *Hum. Mol. Genet.* **12**, 3215–3223.
14. Kim, H.Y., and Gladyshev, V.N. (2004). Characterization of mouse endoplasmic reticulum methionine-R-sulfoxide reductase. *Biochem. Biophys. Res. Commun.* **320**, 1277–1283.
15. Novoselov, S.V., Kim, H.Y., Hua, D., Lee, B.C., Astle, C.M., Harrison, D.E., Friguet, B., Moustafa, M.E., Carlson, B.A., Hatfield, D.L., and Gladyshev, V.N. (2010). Regulation of selenoproteins and methionine sulfoxide reductases A and B1 by age, calorie restriction, and dietary selenium in mice. *Antioxid. Redox Signal.* **12**, 829–838.
16. Van Eyken, E., Van Camp, G., Fransen, E., Topsakal, V., Hendrickx, J.J., Demeester, K., Van de Heyning, P., Mäki-Torkko, E., Hannula, S., Sorri, M., et al. (2007). Contribution of the N-acetyltransferase 2 polymorphism NAT2\*6A to age-related hearing impairment. *J. Med. Genet.* **44**, 570–578.
17. Van Eyken, E., Van Laer, L., Fransen, E., Topsakal, V., Hendrickx, J.J., Demeester, K., Van de Heyning, P., Mäki-Torkko, E., Hannula, S., Sorri, M., et al. (2007). The contribution of GJB2 (Connexin 26) 35delG to age-related hearing impairment and noise-induced hearing loss. *Otol. Neurotol.* **28**, 970–975.
18. Fransen, E., Van Laer, L., Lemkens, N., Caethoven, G., Flothmann, K., Govaerts, P., Van de Heyning, P., and Van Camp, G. (2004). A novel Z-score-based method to analyze candidate genes for age-related hearing impairment. *Ear Hear.* **25**, 133–141.
19. Huyghe, J.R., Van Laer, L., Hendrickx, J.J., Fransen, E., Demeester, K., Topsakal, V., Kunst, S., Manninen, M., Jensen, M., Bonaconsa, A., et al. (2008). Genome-wide SNP-based linkage scan identifies a locus on 8q24 for an age-related hearing impairment trait. *Am. J. Hum. Genet.* **83**, 401–407.
20. Kim, H.Y., and Gladyshev, V.N. (2004). Methionine sulfoxide reduction in mammals: Characterization of methionine-R-sulfoxide reductases. *Mol. Biol. Cell* **15**, 1055–1064.
21. Weissbach, H., Etienne, F., Hoshi, T., Heinemann, S.H., Lowther, W.T., Matthews, B., St John, G., Nathan, C., and Brot, N. (2002). Peptide methionine sulfoxide reductase: structure, mechanism of action, and biological function. *Arch. Biochem. Biophys.* **397**, 172–178.
22. Kim, H.Y., and Gladyshev, V.N. (2005). Different catalytic mechanisms in mammalian selenocysteine- and cysteine-containing methionine-R-sulfoxide reductases. *PLoS Biol.* **3**, e375.
23. Zheng, Q.Y., Ding, D., Yu, H., Salvi, R.J., and Johnson, K.R. (2009). A locus on distal chromosome 10 (ahl4) affecting age-related hearing loss in A/J mice. *Neurobiol. Aging* **30**, 1693–1705.
24. Davis, A. (1994). Prevalence of hearing impairment. In *Hearing in Adults*, A. Davis, ed. (London: Whurr Publishers Ltd), pp. 43–321.
25. Friedman, R.A., Van Laer, L., Huentelman, M.J., Sheth, S.S., Van Eyken, E., Corneveaux, J.J., Tembe, W.D., Halperin, R.F., Thorburn, A.Q., Thys, S., et al. (2009). GRM7 variants confer susceptibility to age-related hearing impairment. *Hum. Mol. Genet.* **18**, 785–796.
26. Van Laer, L., Van Eyken, E., Fransen, E., Huyghe, J.R., Topsakal, V., Hendrickx, J.J., Hannula, S., Mäki-Torkko, E., Jensen, M., Demeester, K., et al. (2008). The grainyhead like 2 gene (GRHL2), alias TFCP2L3, is associated with age-related hearing impairment. *Hum. Mol. Genet.* **17**, 159–169.

27. Moskovitz, J., Bar-Noy, S., Williams, W.M., Requena, J., Berlett, B.S., and Stadtman, E.R. (2001). Methionine sulfoxide reductase (MsrA) is a regulator of antioxidant defense and lifespan in mammals. *Proc. Natl. Acad. Sci. USA* **98**, 12920–12925.
28. Hansel, A., Heinemann, S.H., and Hoshi, T. (2005). Heterogeneity and function of mammalian MSRs: Enzymes for repair, protection and regulation. *Biochim. Biophys. Acta* **1703**, 239–247.
29. Huang, T., Cheng, A.G., Stupak, H., Liu, W., Kim, A., Staecker, H., Lefebvre, P.P., Malgrange, B., Kopke, R., Moonen, G., and Van De Water, T.R. (2000). Oxidative stress-induced apoptosis of cochlear sensory cells: Otoprotective strategies. *Int. J. Dev. Neurosci.* **18**, 259–270.
30. Morishita, H., Makishima, T., Kaneko, C., Lee, Y.S., Segil, N., Takahashi, K., Kuraoka, A., Nakagawa, T., Nabekura, J., Nakayama, K., and Nakayama, K.I. (2001). Deafness due to degeneration of cochlear neurons in caspase-3-deficient mice. *Biochem. Biophys. Res. Commun.* **284**, 142–149.
31. De Martinis, M., Franceschi, C., Monti, D., and Ginaldi, L. (2007). Apoptosis remodeling in immunosenescence: Implications for strategies to delay ageing. *Curr. Med. Chem.* **14**, 1389–1397.
32. Coling, D., Chen, S., Chi, L.H., Jamesdaniel, S., and Henderson, D. (2009). Age-related changes in antioxidant enzymes related to hydrogen peroxide metabolism in rat inner ear. *Neurosci. Lett.* **464**, 22–25.
33. Gabbita, S.P., Aksenov, M.Y., Lovell, M.A., and Markesbery, W.R. (1999). Decrease in peptide methionine sulfoxide reductase in Alzheimer's disease brain. *J. Neurochem.* **73**, 1660–1666.
34. Jiang, H., Talaska, A.E., Schacht, J., and Sha, S.H. (2007). Oxidative imbalance in the aging inner ear. *Neurobiol. Aging* **28**, 1605–1612.
35. Liu, F., Hindupur, J., Nguyen, J.L., Ruf, K.J., Zhu, J., Schieler, J.L., Bonham, C.C., Wood, K.V., Davison, V.J., and Rochet, J.C. (2008). Methionine sulfoxide reductase A protects dopaminergic cells from Parkinson's disease-related insults. *Free Radic. Biol. Med.* **45**, 242–255.
36. Someya, S., Xu, J., Kondo, K., Ding, D., Salvi, R.J., Yamasoba, T., Rabinovitch, P.S., Weindruch, R., Leeuwenburgh, C., Tanokura, M., and Prolla, T.A. (2009). Age-related hearing loss in C57BL/6J mice is mediated by Bak-dependent mitochondrial apoptosis. *Proc. Natl. Acad. Sci. USA* **106**, 19432–19437.
37. Walss-Bass, C., Soto-Bernardini, M.C., Johnson-Pais, T., Leach, R.J., Ontiveros, A., Nicolini, H., Mendoza, R., Jerez, A., Dassori, A., Chavarria-Siles, I., et al. (2009). Methionine sulfoxide reductase: a novel schizophrenia candidate gene. *Am. J. Med. Genet. B. Neuropsychiatr. Genet.* **150B**, 219–225.
38. Wassef, R., Haenold, R., Hansel, A., Brot, N., Heinemann, S.H., and Hoshi, T. (2007). Methionine sulfoxide reductase A and a dietary supplement S-methyl-L-cysteine prevent Parkinson's-like symptoms. *J. Neurosci.* **27**, 12808–12816.
39. Beatty, S., Koh, H., Phil, M., Henson, D., and Boulton, M. (2000). The role of oxidative stress in the pathogenesis of age-related macular degeneration. *Surv. Ophthalmol.* **45**, 115–134.
40. Hollyfield, J.G., Bonilha, V.L., Rayborn, M.E., Yang, X., Shadrach, K.G., Lu, L., Ufret, R.L., Salomon, R.G., and Perez, V.L. (2008). Oxidative damage-induced inflammation initiates age-related macular degeneration. *Nat. Med.* **14**, 194–198.
41. Jarrett, S.G., Lin, H., Godley, B.F., and Boulton, M.E. (2008). Mitochondrial DNA damage and its potential role in retinal degeneration. *Prog. Retin. Eye Res.* **27**, 596–607.
42. Marchetti, M.A., Pizarro, G.O., Sagher, D., Deamicis, C., Brot, N., Hejtmancik, J.F., Weissbach, H., and Kantorow, M. (2005). Methionine sulfoxide reductases B1, B2, and B3 are present in the human lens and confer oxidative stress resistance to lens cells. *Invest. Ophthalmol. Vis. Sci.* **46**, 2107–2112.
43. Truscott, R.J. (2005). Age-related nuclear cataract-oxidation is the key. *Exp. Eye Res.* **80**, 709–725.
44. Kumar, R.A., Koc, A., Cerny, R.L., and Gladyshev, V.N. (2002). Reaction mechanism, evolutionary analysis, and role of zinc in *Drosophila* methionine-R-sulfoxide reductase. *J. Biol. Chem.* **277**, 37527–37535.
45. Olry, A., Boschi-Muller, S., Yu, H., Burnel, D., and Branlant, G. (2005). Insights into the role of the metal binding site in methionine-R-sulfoxide reductases B. *Protein Sci.* **14**, 2828–2837.
46. Jin, H., May, M., Tranebjaerg, L., Kendall, E., Fontan, G., Jackson, J., Subramony, S.H., Arena, F., Lubs, H., Smith, S., et al. (1996). A novel X-linked gene, DDP, shows mutations in families with deafness (DFN-1), dystonia, mental deficiency and blindness. *Nat. Genet.* **14**, 177–180.
47. Tranebjaerg, L., Hamel, B.C., Gabreels, F.J., Renier, W.O., and Van Ghelue, M. (2000). A de novo missense mutation in a critical domain of the X-linked DDP gene causes the typical deafness-dystonia-optic atrophy syndrome. *Eur. J. Hum. Genet.* **8**, 464–467.
48. Roesch, K., Hynds, P.J., Varga, R., Tranebjaerg, L., and Koehler, C.M. (2004). The calcium-binding aspartate/glutamate carriers, citrin and aralar1, are new substrates for the DDP1/TIMM8a-TIMM13 complex. *Hum. Mol. Genet.* **13**, 2101–2111.
49. Koehler, C.M., Leuenberger, D., Merchant, S., Renold, A., Junne, T., and Schatz, G. (1999). Human deafness dystonia syndrome is a mitochondrial disease. *Proc. Natl. Acad. Sci. USA* **96**, 2141–2146.